HHS Public Access

Author manuscript

Exp Cell Res. Author manuscript; available in PMC 2020 January 01.

Published in final edited form as:

Exp Cell Res. 2019 January 01; 374(1): 128–139. doi:10.1016/j.yexcr.2018.11.017.

VANGL2 protein stability is regulated by integrin αv and the extracellular matrix

Tammy N. Jessen and **Jason R. Jessen***

Department of Biology, Middle Tennessee State University, Murfreesboro, TN, USA.

Abstract

Vang-like 2 (VANGL2) is a four-pass transmembrane protein required for a variety of polarized cell behaviors underlying embryonic development. Recent data show human VANGL2 interacts with integrin αv to control cell adhesion to extracellular matrix proteins. The goal of this study was to further define the functional relationship between integrin αv and VANGL2. We demonstrate integrin αv regulates VANGL2 protein levels both *in vitro* and in the zebrafish embryo. While integrin αv knockdown reduces VANGL2 expression at membrane compartments, it does not affect *VANGL2* transcription. Knockdown of integrin β5, but not β1 or β3, also decreases VANGL2 protein levels. Inhibition of protein translation using cycloheximide demonstrates that integrin αv knockdown cells have increased VANGL2 degradation while interference with either proteasome or lysosome function restores VANGL2. We further show integrin activation and stimulation of cell-matrix adhesion using $MnCl_2$ fails to influence VANGL2. However, $MnCl_2$ treatment stabilizes VANGL2 protein expression levels in the presence of cycloheximide. In the converse experiment, blockage of integrin-mediated cell-matrix adhesion using a cyclic RGD peptide causes a reduction in VANGL2 protein levels. Together, our findings support a model where integrin αv and cellular interactions with the extracellular matrix are required to maintain VANGL2 protein levels and thus function at the plasma membrane.

Keywords

VANGL2; integrin αv; protein stability; extracellular matrix; adhesion

1. Introduction

The Van Gogh protein was first identified as a regulator of planar cell polarity (PCP) in *Drosophila melanogaster* [1, 2]. Vertebrate homologs of fly Van Gogh, Vang-like 1 and 2 (VANGL1/2), are linked to several morphogenetic processes including polarized cell movements associated with neural tube closure and gastrulation [3]. VANGL proteins are

*Corresponding author: Jason R. Jessen, address: Middle Tennessee State University, Department of Biology, P.O. Box 60, Murfreesboro, TN 37132. telephone: (615) 898-2060. jason.jessen@mtsu.edu.

Conflicts of interest

None declared.

also linked to tumor cell migration and invasion [4]. In regard to PCP, VANGL2 functions as part of a network of core signaling proteins that includes Prickle, Dishevelled, Frizzled, Diego/ANKRD, and Flamingo/CELSR. In the fly, asymmetric plasma membrane PCP protein expression underlies the propagation of a polarity signal between cells that results in establishment of polarity across tissues [5]. Loss of mouse Vangl2 function causes a severe defect where the neural tube remains open from the hindbrain to the tail [6, 7]. Nonsynonymous mutations in human *VANGL* genes also produce neural tube defects [8]. For the zebrafish gastrula, PCP is manifested as the elongation and mediolateral alignment of ectodermal and mesodermal cells perpendicular to the dorsal body axis [9, 10]. Zebrafish *vangl2* mutations disrupt the gastrulation movements of convergence and extension and produce embryos that are mediolaterally broadened and have shorter anterior/posterior body axes [9, 11, 12]. Given the many roles of VANGL2 homologs during embryonic morphogenesis and disease processes, it has become increasingly important to understand their function and regulation.

Structurally, VANGL proteins have four transmembrane domains with both amino and carboxyl termini oriented toward the cytoplasm [13] and involved in binding proteins such as Dishevelled and Prickle [14, 15]. Plasma membrane expression is required for VANGL function and is regulated by multiple proteins. Sec24b mediates the transport of mouse Vangl2 in COPII-coated vesicles from the endoplasmic reticulum to the Golgi and mutations in *Sec24b* produce neural tube closure phenotypes similar to those caused by disruption of *Vangl2* [16]. Trafficking of Vangl2 from the trans-Golgi network is controlled by a combination of Arf GTP-binding and clathrin adaptor complex proteins [17]. Data suggest that Vangl2 and Frizzled6 are packaged into different vesicles in the trans-Golgi network and it is thought this may promote asymmetric localization at the cell surface [18].

Published data describe missense mutations in mouse *Vangl1* that affect protein stability and plasma membrane localization. Here, misfolded mutant Vangl1 proteins are retained within the endoplasmic reticulum until they are transported to the cytosol and selectively degraded in a proteasome-dependent manner [19, 20]. In addition to asymmetric delivery of VANGL2 to specific subcellular plasma membrane domains, asymmetric VANGL2 distribution may be achieved through regulation of cell surface protein stability [21]. As a cell surface protein, VANGL2 function can be regulated by endocytosis and degradation in lysosomal compartments. Indeed, inhibition of lysosomal enzymes increases the level of mouse Vangl2 protein [22]. Mechanistically, current data from mouse suggest that Wnt5a signaling can increase Vangl2 protein stability at the plasma membrane by promoting the binding of Vangl2 with the receptor-like tyrosine kinase Ryk [22].

Previous results from tissue culture, frog, and zebrafish have identified relationships between PCP proteins and the extracellular matrix (ECM) [15, 23–25]. In these reports manipulation of VANGL2/Vangl2 function disrupts assembly of a fibrillar fibronectin ECM. For example, knockdown of human VANGL2 in HT-1080 fibrosarcoma cells increases activation of matrix metalloproteinase 2 (MMP2) and invasiveness through ECM substrates [23, 26]. VANGL2 influences integrin-mediated adhesion to the ECM and VANGL2-dependent regulation of MMP2 activation requires integrin αv [26]. Loss of zebrafish Vangl2 also increases protease activity and produces embryos with reduced fibronectin [23, 25].

Conversely, knockdown of fibronectin during zebrafish gastrulation causes a reduction in cell surface Vangl2 [27] suggesting that the ECM and perhaps integrin-dependent cell-matrix interactions regulate Vangl2 protein levels. Here we use tissue culture experiments to provide evidence that integrin αv and cell-matrix adhesion function to maintain human VANGL2 protein stability at membranes.

2. Materials and methods

2.1. Cell culture and siRNA and plasmid DNA transfection

HT-1080 cells were obtained from the American Type Culture Collection (Manassas, VA, USA) and maintained as previously described [26]. Cells were seeded overnight in multiwell plates and transfected with siRNA at 40–50% confluence using DharmaFECT 4 lipid reagent (Dharmacon Inc., Lafayette, CO). The following siRNAs were used: Dharmacon SiGenome SMARTpool human PRICKLE1 (M-016677); Thermo Fisher Scientific Silencer Select human VANGL1 (S37813); Dharmacon ON-TARGETplus SMARTpool human VANGL2 (L-010581), integrin αv (L-004565), integrin α5 (L-008003), integrin β1 (L-004506), integrin β3 (L-004124), and integrin β5 (L-004125) siRNAs; Dharmacon human integrin αv single siRNAs (J-004565–08 and J-004565–10); Dharmacon Non-Targeting #2 ON-TARGETplus SMARTpool Control siRNA (D-001810). The siRNA pools were used at 100 nM while the single siRNAs were used at 25 nM. For all siRNA experiments, cells were transfected 4 days and protein knockdown was confirmed using western blot. The integrin αv siRNA pool was used throughout this study except as noted in Fig. 1. VANGL2 expression was visualized using a plasmid containing full-length human VANGL2 fused to GFP (GFP-VANGL2). Plasmid transfection was performed as previously described [26].

2.2. Quantitative RT-PCR

Cells were seeded in multiwell plates and transfected with control Non-Targeting and integrin αv siRNA as described above. Total RNA was isolated and cDNA synthesized using standard methods. PCR reactions were run using TaqMan probes and TaqMan Fast Advanced Master Mix (Applied Biosystems, Foster City, CA) for either *VANGL2* or *hypoxanthine phosphoribosyltransferase 1* (*HPRT1*) following the manufacturer's instructions. Quantitative PCR was run on a Bio-Rad CFX96 Touch Real-Time machine and data analyzed using CFX Maestro software. Delta Ct values were calculated as described [28, 29].

2.3. Zebrafish husbandry and morpholino microinjection

Wild-type (strain AB* and TL) adult zebrafish (*Danio rerio*) 1–2 years of age were maintained following standard procedures [30]. Embryos were collected after natural spawnings and grown at 28.5°C in purified water containing 60 mg/L Instant Ocean. Single-cell stage embryos were injected with 5–10 ng of antisense morpholino oligonucleotides following standard procedures [31]. Morpholinos were provided by Gene Tools, LLC (Eugene, OR): *integrin αv*, 5'-cggacgaagtgtttgcccatgtttt-3' [32]; standard control oligo, 5'-cctcttacctcagttacaatttata-3'.

The Middle Tennessee State University Institutional Animal Care and Use Committee approved the animal research described in this paper. All procedures were conducted following approved National Institutes of Health guidelines. The Office of Laboratory Animal Welfare assurance number is A4701–01.

2.4. Biotinylation, cell fractionation, western blot and antibodies

For cell surface biotinylation, HT-1080 cells were seeded in 6-well plates and transfected with siRNAs as described above. On day 4 post-transfection, the plates were washed with ice-cold PBS (pH 8.0) and incubated for 15 min. The PBS was removed and replaced with 1 mg/ml EZ-Link Sulfo-NHS-LC-Biotin (Thermo Fisher Scientific) and the plates were incubated for 10 min followed by two washes with ice-cold PBS. Next, PBS containing 100 mM glycine was added to the wells and the plates incubated for 20 min followed by three more washes with PBS. The samples were kept on ice throughout the procedure. Protein was solubilized using RIPA lysis buffer containing a protease inhibitor cocktail. Streptavidin M-280 Dynabeads (Thermo Fisher Scientific) were used as directed to bind biotinylated proteins in whole cell lysates. Cellular protein fractionation was performed using a kit as described by the manufacturer (78840, Thermo Fisher Scientific). After quantification using the BCA assay, proteins were denatured in Laemmli sample buffer containing β□mercaptoethanol at 95°C for 5 min.

Non-biotinylated and non-cell fractionated total protein was extracted from HT-1080 cells and 24 h post-fertilization zebrafish embryos and quantified as previously described [15, 26]. Protein lysates were separated by 10% SDS-PAGE under reducing conditions and transferred to PVDF membranes using a Trans-Blot Turbo (Bio-Rad, Hercules, CA). Non-specific binding was blocked with TBS-Tween (50 mM Tris, pH 7.4, 150 mM NaCl, 0.1% Tween-20) containing 0– 5% non-fat milk depending on the antibody used and membranes were incubated overnight at 4°C with primary antibody in block solution. Membranes were incubated with peroxidase-conjugated affinity-purified donkey anti-rabbit, anti-mouse, or anti-rat secondary antibodies (Jackson ImmunoResearch Laboratories, Inc., West Grove, PA). Blots were developed using Clarity Chemiluminescent Substrate (Bio-Rad) and imaged using a UVP GelDoc-It Imaging System (Upland, CA). In each experiment blots were stripped at room temperature for 15 min using 25 mM glycine and 1% SDS (pH 2.0) and re-probed with GAPDH or actin antibodies. The primary antibodies were VANGL2 (1:1000, MABN750), Millipore Sigma, St. Louis, MO; integrin αv (1:1000, ab17975), integrin β1 (1:1000, ab30394), and pan-cadherin (1:1000, ab16505) Abcam, Cambridge, MA; integrin α5 (1:1000, #4705), integrin β5 (1:1000, #3629), integrin β3 (1:1000, #13166), and β-actin (1:1000, #4967), Cell Signaling Technology, Danvers, MA; GAPDH-HRP (1:2000, GTX627408–01), GeneTex, Inc., Irvine, CA. Densitometry was performed on blots using UVP Visionworks software. For western blots, the experimental bands were normalized using GAPDH or actin controls.

2.5. Coating plates and coverslip dishes with ECM proteins

Recombinant human vitronectin (SRP3186, Millipore Sigma) was reconstituted for a stock solution of 100 μg/ml. Working solutions (1 μg/cm^2) were made in PBS and applied for 2 h at room temperature then overnight at 4°C as directed. Prior to use, excess vitronectin was

removed without washing. Human fibronectin (#354008, Corning, Corning, NY) was reconstituted for a stock solution of 1 mg/ml. Working solutions (1 μg/cm^2) were made in PBS and applied for 1 h at 37°C then overnight at 4°C as directed. Excess fibronectin was removed with gentle PBS washing.

2.6. Protein stability and drug treatment

Cycloheximide (#2112), MG-132 (#2194), and chloroquine (#14774) were purchased from Cell Signaling Technology. On day 4 post-siRNA transfection cells were treated as follows: DMSO (control), cycloheximide (20 μg/ml), MG-132 (5 μg/ml)/cycloheximide (20 μg/ml), and chloroquine (100 μM)/cycloheximide (20 μg/ml). Unless otherwise indicated, cells were incubated for 6 h at 37°C in 5% CO_2 before total protein extraction. Drug concentrations and incubation times were chosen based on a previous publication examining Vangl1 protein stability [19].

2.7. Cell-adhesion assays, integrin activation, and RGD peptide treatment

Cellular adhesion to ECM proteins was assayed as previously described [26]. Here, detached cells were treated with 1 mM $MnCl_2$ or 0.1, 1, and 10 μM cyclic RGD peptide (cilengitide trifluoroacetic acid salt, SML1594, Millipore Sigma). No difference in cell viability was observed between 0.1, 1, and 10 μM cyclic RGD peptide treatment. Cells were allowed to adhere in a humidified 37°C CO_2 incubator for 60 min prior to washing and staining with a 0.2% crystal violet solution and microplate reader absorbance analysis (560 nm). For western blot experiments, cells were plated in complete media on plastic, vitronectin, or fibronectin at a cell concentration that would reach confluence within 24 h. For some experiments, the media was replaced with complete media containing 1 mM $MnCl_2$ and the cells incubated 2 h at 37°C in 5% CO_2 before total protein extraction. Alternatively, cells were treated with non-enzymatic dissociation buffer and suspended in media containing 10 μM cyclic RGD peptide before seeding on vitronectin or fibronectin coated plates. These cells were incubated overnight at 37°C in 5% CO_2 before total protein extraction.

2.8. Immunofluorescence and imaging

Non-transfected or GFP-VANGL2 transfected HT-1080 cells were plated on vitronectin or fibronectin treated coverslip dishes. Cells were left untreated or treated with $MnCl_2$ and fixed using 4% paraformaldehyde/PBS at room temperature or ice-cold methanol at −20°C. Washed cells were blocked using PBS, 5% normal donkey serum, and 0.1% Triton X-100 for 1 h at room temperature. Cells were incubated with LAMP1 (1:100, D2D11 XP; Cell Signaling Technology), fibronectin (1:100, F3648, Millipore Sigma), paxillin (1:100, AHO0492, Thermo Fisher), or integrin αv (1:100, ab179475, Abcam) primary antibody in block for 1 h at room temperature, washed twice with PBS, and incubated an additional 1 h in the dark with Donkey anti-Rabbit or anti-mouse Alex Fluor 594 (1:500, 711–585-152/715–585-150; Jackson ImmunoResearch Laboratories). Cells were washed three times with PBS. NucBlue Fixed Cell DAPI Stain (Thermo Fisher Scientific) was used to label nuclei. Imaging was performed using a 40x oil objective (NA = 1.3) or 20x dry objective (NA = 0.75) and an Olympus IX83 inverted microscope equipped with a Hamamatsu Orca Flash 4.0 camera. For some images, maximum intensity projections were generated from z-stack slices (0.5 μm).

2.9. Data analysis and statistics

Experiments were repeated at least three times and the total number of biological replicates is listed in each figure legend. Graphing and statistical analyses were performed using GraphPad Prism 6 software (GraphPad Software, La Jolla, CA). The data are normally distributed and a two-tailed unpaired Student's t-test was used for analysis. Box and whisker plots were used for graphing purposes except for Fig. 1D (scatter plot). Standard deviations for the control samples were obtained by dividing individual control data values by the average of the sum of all control data values. Dividing individual experimental data values by the average of the control data values and multiplying by one hundred was done to obtain the percent of control values. Western blot and immunofluorescence images shown are representative of each experiment.

3. Results and discussion

3.1. Integrin αv knockdown reduces VANGL2 protein levels in vitro and in zebrafish

We previously showed that siRNA-mediated knockdown of VANGL2 in HT-1080 cells disrupts plasma membrane expression of integrin αv [26]. To further address the relationship between VANGL2 and integrin function, we again used HT-1080 cells to perform the converse experiment. Cells were transfected with integrin αv siRNA and total VANGL2 protein levels were analyzed using western blot. We first verified that integrin αv knockdown affects both cell surface and cytoplasmic integrin protein expression (Fig. 1A). Three different integrin αv siRNA treatments were then compared, each of which has a different effect on integrin αv protein knockdown (Fig. 1B) [26]. Our results show integrin αv siRNA transfected cells have a reduced level of VANGL2 protein correlating with the efficacy of integrin αv knockdown (Fig. 1C,D). We next performed quantitative RT-PCR to test whether the observed reduction in VANGL2 protein in integrin αv knockdown cells was due to transcriptional down-regulation. Our data show that *VANGL2* mRNA expression is unchanged in integrin αv siRNA transfected cells compared to controls (Fig. 1E). In HT-1080 cells and zebrafish gastrula cells VANGL2/Vangl2 localizes to the plasma membrane and intracellular vesicles [25, 27, 33]. VANGL proteins have just 33 non-lysine extracellular amino acids [13] making standard biotinylation and antibody-based flow cytometry methods ineffective. However, we confirmed that integrin αv knockdown reduces VANGL2 protein levels in membrane compartments (plasma and intracellular) using cellular fractionation and western blot (Supplementary Fig. 1). To determine whether integrin αv alters cell surface VANGL2 protein levels, integrin αv knockdown was performed on GFP-VANGL2 expressing cells. We report a consistent and marked loss of GFP-VANGL2 expression from the plasma membrane and to a lesser extent from the cytoplasm (Fig. 1F and Fig. 6). Taken together, these data demonstrate that integrin αv is required to maintain VANGL2 protein levels in HT-1080 cells including expression at the cell surface. Depending on cell type, plasma membrane integrin αv can localize to focal adhesion structures [34] where it interacts with β integrin proteins to bind ECM substrates. We found that while GFP-VANGL2 overlaps with integrin αv and paxillin at the plasma membrane of HT-1080 cells, it exhibits little or no expression in mature focal adhesions (Fig. 2A,B). Though further experiments are needed, these *in vitro* findings suggest that integrin αv-dependent regulation of VANGL2 may occur at sites of weak or transient cell-matrix adhesion. Previous data

show that loss of VANGL2 in HT-1080 cells affects the number and perhaps distribution of paxillin-positive focal adhesions [25].

To expand upon the *in vitro* data, we next investigated whether zebrafish integrin αv influences Vangl2 protein levels *in vivo*. During zebrafish embryogenesis, *integrin αv* and *vangl2* exhibit overlapping mRNA expression patterns during multiple stages beginning at gastrulation. We used a previously validated *integrin αv* antisense morpholino oligonucleotide to knockdown endogenous protein expression. Validated refers to the ability of injected synthetic zebrafish *integrin αv* mRNA (that is not targeted by the morpholino) to suppress *integrin αv* morpholino phenotypes [35]. Wild-type embryos were injected at the single-cell stage with control or *integrin αv* morpholinos to achieve ubiquitous oligonucleotide distribution and total protein was prepared at 24 h post-fertilization. At this stage of development, *vangl2* and *integrin αv* both exhibit broad mRNA expression in forebrain, midbrain, and hindbrain tissues [36, 37]. Consistent with our *in vitro* data, western blot analysis showed *integrin αv* morpholino injected zebrafish embryos have reduced total Vangl2 protein (Fig. 3A,B). Despite both *vangl2* and *integrin αv* being expressed in gastrula-stage embryos, we did not observe the obvious convergence and extension phenotype typically associated with *vangl2* mutant embryos [9, 12]. Future research will address in more detail how these proteins interact during zebrafish gastrulation. Interestingly, both integrin αv and Vangl2 are linked to the formation and function of Kupffer's vesicle, a ciliated organ that regulates asymmetry during zebrafish gastrulation [35, 38, 39]. It will also be important to identify additional embryonic stages and specific cell types where Vangl2 protein levels are regulated by integrin αv.

3.2. Specificity of the integrin αv phenotype and VANGL2 regulation by β integrins

HT-1080 cells express other PCP proteins including the VANGL2 binding partner PRICKLE1 and the VANGL2 homolog VANGL1 [23]. Therefore we tested whether integrin αv knockdown influences the levels of these proteins. Our results show the expression of PRICKLE1 and VANGL1 are unaffected by a reduction in integrin αv (Supplementary Fig. 2A,B). PRICKLE1 is a cytoplasmic polarity protein that is likely recruited to the plasma membrane through its physical interaction with VANGL2 [14]. Given the effect of integrin αv on VANGL2, it is possible integrin αv knockdown disrupts the subcellular distribution of PRICKLE1 but not total protein levels. VANGL1 and VANGL2 proteins share 73% sequence identity and 85% sequence similarity. During embryonic development, VANGL proteins have distinct and overlapping functions. For example, while both VANGL1 and VANGL2 are required for neural tube closure [40, 41], zebrafish *vangl1* is not expressed during gastrulation, an embryonic stage where Vangl2 function is essential [9, 12, 37]. The lack of an effect by integrin αv on VANGL1 supports the notion that VANGL2 can be regulated differently than VANGL1. Notably, although VANGL1 was shown to modulate MMP3 expression and cell invasiveness through an ECM [42], we were unable to identify published data connecting VANGL1 and integrin function.

Similar to integrin αv, integrin α5 also interacts with specific β integrin proteins to allow cell adhesion to RGD motif-containing ECM proteins including fibronectin [43]. In contrast to integrin αv, we find that HT-1080 cells transfected with integrin α5 siRNA exhibit normal

levels of VANGL2 protein (Supplementary Fig. 2C,D). HT-1080 cells express several β integrins [26, 44, 45] that may function with integrin αv to control VANGL2 protein levels. We used siRNA transfection to examine the effects of integrin β1, β3, and β5 protein knockdown on VANGL2. The western blot data show that similar to integrin α5 knockdown, loss of integrin β1 does not affect VANGL2 (Supplementary Fig. 2E,F). By contrast, we found that integrin β3 knockdown increases VANGL2 protein levels (Fig. 4A,B) and loss of integrin β5 decreases VANGL2 (Fig. 4C,D). The latter data suggest that integrin αvβ5 heterodimers may be responsible for promoting VANGL2 stability in HT-1080 cells. The integrin β3 data support the notion that the normal function of this integrin is to decrease VANGL2 protein expression. We hypothesize that VANGL2 regulation is determined by integrin heterodimer identity and the spatiotemporal requirement for these proteins to control specific cell behaviors such as adhesion to the ECM.

3.3. Integrin αv regulates VANGL2 protein degradation

Because integrin αv is required for proper VANGL2 protein expression but does not significantly affect *VANGL2* transcription, we hypothesized that integrin αv may regulate VANGL2 protein homeostasis. To address this we first examined the degradation of endogenously expressed VANGL2 using cycloheximide to inhibit protein synthesis [46]. We show VANGL2 protein levels are already reduced after 4 h of drug treatment (Fig. 5A). Next, the effect of 6 h cycloheximide treatment was assessed on control or integrin αv siRNA transfected cells. Drug treatment reduced the total levels of VANGL2 protein in both control and integrin αv siRNA transfected cells. However, our data show the ratio of VANGL2 protein in cycloheximide treated versus untreated cells is significantly lower in integrin αv knockdown cells compared to controls (Fig. 5B,C). These results indicate that when integrin αv levels are lowered, VANGL2 protein degradation increases. We next tested whether this VANGL2 protein phenotype is rescued by pharmacological inhibition of either the proteasome or lysosome. Here, control and integrin αv siRNA transfected cells were treated with a combination of cycloheximide and either MG-132 (proteasomal enzyme inhibitor) or chloroquine (lysosomal enzyme inhibitor). Our data demonstrate that reduced VANGL2 protein in integrin αv knockdown cells was rescued by inhibition of either the proteasome or lysosome (Fig. 5C,D). To examine lysosomal regulation of VANGL2 further, we again used GFP-VANGL2 to image protein localization. Plasmid DNA and siRNA transfected HT-1080 cells were fixed and co-labeled with the lysosomal-associated membrane protein LAMP1. This transmembrane glycoprotein localizes primarily to late endosomes and lysosomes [47]. In control cells, GFP-VANGL2 is detected in both vesicular and plasma membrane domains (Fig. 6A,a'). When integrin αv is knocked down, GFP-VANGL2 shows a marked reduction in plasma membrane expression but maintains its localization in sub-populations of LAMP1-positive (Fig. 6B,b' and 6C,c') and early endosome antigen 1-positive (Supplementary Fig. 3A,B) endosomes. Together, our results support the notion that VANGL2 protein is degraded by both proteasomal- and lysosomal-dependent mechanisms and that integrin αv acts to stabilize VANGL2 protein levels by preventing this degradation.

Like other cell surface transmembrane proteins, VANGL2 is initially inserted into the lipid bilayer in the endoplasmic reticulum and trafficked to the plasma membrane from the trans-

Golgi network. As shown for mouse Vangl1 [19, 20], misfolded VANGL2 proteins would retro-translocate from the endoplasmic reticulum to the cytosol for degradation by the proteasome. Once at the cell surface, misfolded VANGL2 might be degraded by the proteasome through a Derlin-dependent quality control mechanism [48, 49] or ubiquitinated and trafficked to lysosomes for degradation by acid hydrolases [50]. While it is unlikely integrin αv knockdown increases the amount of misfolded VANGL2 in the endoplasmic reticulum, it may affect the stability of VANGL2 tertiary or quaternary structure at the plasma membrane. Vertebrate VANGL2 homologs bind several plasma membrane proteins that may influence conformational stability including integrin αv, N-cadherin, and Ryk [22, 26, 51]. Our current data do not distinguish between MG-132 treatment directly affecting proteasomal VANGL2 degradation or indirectly disrupting the ubiquitination and endocytic trafficking of VANGL2 to lysosomes [52, 53]. Besides the removal of misfolded protein or misassembled protein complexes, endolysosomal vesicular trafficking may also provide a mechanism to down-regulate properly folded and functional plasma membrane VANGL2. Though lysosomal enzyme inhibition rescues VANGL2 protein levels in integrin αv knockdown cells, it is unclear whether integrin αv regulates lysosomal degradation of functional or defective cell surface VANGL2.

3.4. VANGL2 protein levels are influenced by the ECM substrate

Integrins function as cell surface receptors for diverse ECM proteins. Through interactions with different β subunits, integrin αv can bind multiple substrates including the RGD-containing ECM proteins fibronectin and vitronectin [54, 55]. The ability of integrin αv to regulate degradation of VANGL2 suggests cellular interactions with the ECM may control VANGL2 protein levels. We therefore compared the quantity of total VANGL2 protein in HT-1080 cells grown on untreated plastic, fibronectin, and vitronectin. Cells were plated on each substrate and incubated for 48 h prior to protein extraction and western blot analysis. Despite possible influences by ECM proteins present in serum [56], our data show that VANGL2 protein is increased in cells grown on fibronectin-coated dishes compared to either untreated plastic or vitronectin-coated dishes (Supplementary Fig. 4). These results are consistent with data from zebrafish showing a relationship between the fibronectin ECM and plasma membrane Vangl2 expression [27]. Similar to human VANGL2, membrane type-1 matrix metalloproteinase (MMP14) is regulated differently when cells are grown on fibronectin versus vitronectin substrates [57]. Here it was proposed that integrin β1 engagement with fibronectin inhibits internalization of MMP14. Further work is needed to determine whether integrin binding to fibronectin prevents VANGL2 endocytosis. The finding that a fibronectin ECM substrate but not vitronectin impacts VANGL2 may indicate involvement of distinct integrin heterodimers. Integrin αvβ3 and αvβ5 bind both fibronectin and vitronectin but other integrin αv heterodimers and integrin α5β1 exhibit selective binding to fibronectin or vitronectin [43, 58, 59]. While our data support the hypothesis that cell-matrix adhesion influences VANGL2 protein levels, these experiments did not specifically address whether cell-fibronectin or cell-vitronectin binding are required to stabilize VANGL2.

3.5. Integrin activation increases VANGL2 protein stability

The ability of integrin αv to influence VANGL2 protein stability may provide a mechanism for cells to regulate VANGL2 function in response to changes in the ECM microenvironment.Our published data confirm that loss of integrin αv function in HT-1080 cells disrupts cell adhesion to ECM proteins [26]. We therefore hypothesized that VANGL2 protein levels may be regulated downstream of integrin binding to the ECM. To explore this possibility we first tested whether integrin activation influences VANGL2 protein expression. It is well established that Mn^{2+} stimulates a shift to a high-affinity integrin conformation that increases cell adhesion to the ECM and assembly of a fibrillar matrix [60]. We used fibronectin antibody labeling and cell adhesion assays to verify the effect of $MnCl_2$ treatment on HT-1080 cells (Fig. 7A,B). We also show that $MnCl_2$ treatment rescues the previously published reduced cell-matrix adhesion phenotype observed with VANGL2 knockdown cells (Fig. 7B) [26]. Although $MnCl_2$ treatment increases both fibronectin assembly and cell-matrix adhesion, integrin activation was insufficient to increase VANGL2 protein levels in cells plated on either fibronectin or vitronectin as indicated by western blot analysis (Fig. 7C-E). $MnCl_2$ treated cells plated on fibronectin actually had slightly reduced VANGL2 (Fig. 7D). These results indicate that further promoting integrin-matrix interactions of cells already adhered to an ECM does not increase VANGL2 protein levels. However, the data do not tell us whether integrin activation functions to stabilize VANGL2. We therefore repeated the cycloheximide protein stability assay and examined the effect of $MnCl_2$ treatment on VANGL2. The ratio of VANGL2 protein in untreated cells versus $MnCl_2$ treated cells was used as an indicator of changes in protein stability. Our data show that $MnCl_2$ treatment rescues VANGL2 protein levels in cycloheximide treated cells (Fig. 7F,G). We interpret these findings as evidence that integrin-mediated cell-matrix adhesion regulates VANGL2 protein stability.

3.6. Inhibition of cell-matrix adhesion reduces VANGL2 protein levels

We next asked whether inhibition of integrin-matrix interactions causes a decrease in VANGL2 protein levels. Here, an Arg-Gly-Asp (RGD) peptide was used to inhibit integrin-binding to RGD-motifs present in certain ECM proteins including fibronectin and vitronectin. We chose a cyclic RGD peptide (cilengitide) because its bent structure is highly selective for the integrin heterodimers examined in our study (IC_{50}-values: αvβ3 < αvβ5 < α5β1 << αvβ6 < αvβ8) [54, 61]. Vitronectin cell adhesion assays were used to confirm RGD peptide efficacy on HT-1080 cells (Fig. 8A). Our data show RGD peptide treated cells plated on vitronectin have a significant decrease in VANGL2 protein (Fig. 8B,C). These results support the notion that VANGL2 protein degradation is inhibited by integrin-mediated cellular interactions with vitronectin. Even though the cyclic RGD peptide inhibits α5β1 [54], we argue the effect on VANGL2 is likely due to disrupted integrin αv function because integrin α5β1 knockdown has no effect on VANGL2 protein levels and integrin α5β1 does not bind vitronectin [43]. It remains possible a complete loss of integrin α5 protein may be required to affect VANGL2 expression.

We found that plating HT-1080 cells on fibronectin increases VANGL2 protein levels whereas plating cells on vitronectin does not. This may simply suggest VANGL2 is regulated by an integrin heterodimer that binds fibronectin but not vitronectin [43, 55, 58,

59]. However, we also show VANGL2 protein levels are affected by RGD peptide treatment when cells are plated on vitronectin but not fibronectin. Integrin heterodimers can exhibit both distinct substrate specificities and distinct substrate binding affinities. For example, published data show the initial binding of integrin αvβ3 is strong for fibronectin but weak for vitronectin [62]. Strong binding to vitronectin requires intracellular signaling events to produce conformational changes in the integrin αvβ3 heterodimer [62, 63]. We hypothesize that integrin-dependent maintenance of VANGL2 protein levels depends on both heterodimer identity and structural conformation as determined by binding different ECM substrates and/or intracellular signaling proteins. VANGL2 protein levels may also be affected by differences in matrix density and stiffness. How might VANGL2 be regulated by integrin αv and cellular interactions with the ECM? Our previous data suggest VANGL2 physically interacts with integrin αv [26]. Therefore differences in integrin-VANGL2 binding affinity, as dictated by the presence or absence of specific ECM substrates or intracellular integrin-binding proteins, may directly maintain VANGL2 at the cell surface. Accumulating data also show trafficking of cell surface integrins can regulate ECM turnover and endocytosis of plasma membrane proteins such as MMP14 [64]. It is possible integrin αv and cell-matrix adhesion directly or indirectly stabilizes plasma membrane VANGL2 by preventing its internalization. We previously reported that VANGL2 is required for cell surface expression of integrin αv [26] suggesting the trafficking of these two proteins may be coordinated. Furthermore, data show that cell surface zebrafish Vangl2 protein localization requires an intact fibronectin ECM [27].

In summary, the current data support a model where integrin αv and cell-matrix interactions function to maintain VANGL2 protein levels including cell surface expression. We propose integrin αv and VANGL2 may interact at plasma membrane domains associated with ECM adhesion to regulate processes such as membrane-protrusive activity. This notion is supported by data showing that both zebrafish Vangl2 and fibronectin are required for proper formation of membrane protrusions in migrating gastrula cells [27].

Supplementary Material

Refer to Web version on PubMed Central for supplementary material.

Acknowledgements

This research was funded by a grant to J.R.J. from the National Institutes of Health (GM102356). Certain laboratory equipment items were provided by Middle Tennessee State University. J.R.J. acknowledges support from the Molecular Biosciences PhD Program and the Department of Biology. The authors thank members of the Jessen lab for helpful discussions and Anna Parnell for technical assistance.

References

[1]. Taylor J, Abramova N, Charlton J, Adler PN, Van Gogh: a new Drosophila tissue polarity gene, Genetics, 150 (1998) 199–210. [PubMed: 9725839]

[2]. Wolff T, Rubin GM, Strabismus, a novel gene that regulates tissue polarity and cell fate decisions in Drosophila, Development, 125 (1998) 1149–1159. [PubMed: 9463361]

[3]. Roszko I, Sawada A, Solnica-Krezel L, Regulation of convergence and extension movements during vertebrate gastrulation by the Wnt/PCP pathway, Semin Cell Dev Biol, 20 (2009) 986–997. [PubMed: 19761865]

[4]. VanderVorst K, Hatakeyama J, Berg A, Lee H, Carraway KL, 3rd, Cellular and molecular mechanisms underlying planar cell polarity pathway contributions to cancer malignancy, Semin Cell Dev Biol, 81 (2018) 78–87. [PubMed: 29107170]

[5]. Strutt DI, The asymmetric subcellular localisation of components of the planar polarity pathway, Semin Cell Dev Biol, 13 (2002) 225–231. [PubMed: 12137731]

[6]. Kibar Z, Vogan KJ, Groulx N, Justice MJ, Underhill DA, Gros P, Ltap, a mammalian homolog of Drosophila Strabismus/Van Gogh, is altered in the mouse neural tube mutant Loop-tail, Nat Genet, 28 (2001) 251–255. [PubMed: 11431695]

[7]. Murdoch JN, Doudney K, Paternotte C, Copp AJ, Stanier P, Severe neural tube defects in the loop-tail mouse result from mutation of Lpp1, a novel gene involved in floor plate specification, Hum Mol Genet, 10 (2001) 2593–2601. [PubMed: 11709546]

[8]. De Marco P, Merello E, Piatelli G, Cama A, Kibar Z, Capra V, Planar cell polarity gene mutations contribute to the etiology of human neural tube defects in our population, Birth Defects Res A Clin Mol Teratol, 100 (2014) 633–641. [PubMed: 24838524]

[9]. Jessen JR, Topczewski J, Bingham S, Sepich DS, Marlow F, Chandrasekhar A, Solnica-Krezel L, Zebrafish trilobite identifies new roles for Strabismus in gastrulation and neuronal movements, Nat Cell Biol, 4 (2002) 610–615. [PubMed: 12105418]

[10]. Topczewski J, Sepich DS, Myers DC, Walker C, Amores A, Lele Z, Hammerschmidt M, Postlethwait J, Solnica-Krezel L, The zebrafish glypican knypek controls cell polarity during gastrulation movements of convergent extension, Dev Cell, 1 (2001) 251–264. [PubMed: 11702784]

[11]. Sepich DS, Myers DC, Short R, Topczewski J, Marlow F, Solnica-Krezel L, Role of the zebrafish trilobite locus in gastrulation movements of convergence and extension, Genesis, 27 (2000) 159–173. [PubMed: 10992326]

[12]. Solnica-Krezel L, Stemple DL, Mountcastle-Shah E, Rangini Z, Neuhauss SC, Malicki J, Schier AF, Stainier DY, Zwartkruis F, Abdelilah S, Driever W, Mutations affecting cell fates and cellular rearrangements during gastrulation in zebrafish, Development, 123 (1996) 67–80. [PubMed: 9007230]

[13]. Iliescu A, Gravel M, Horth C, Apuzzo S, Gros P, Transmembrane topology of mammalian planar cell polarity protein Vangl1, Biochemistry, 50 (2011) 2274–2282. [PubMed: 21291170]

[14]. Bastock R, Strutt H, Strutt D, Strabismus is asymmetrically localised and binds to Prickle and Dishevelled during Drosophila planar polarity patterning, Development, 130 (2003) 3007–3014. [PubMed: 12756182]

[15]. Dohn MR, Mundell NA, Sawyer LM, Dunlap JA, Jessen JR, Planar cell polarity proteins differentially regulate extracellular matrix organization and assembly during zebrafish gastrulation, Dev Biol, 383 (2013) 39–51. [PubMed: 24021482]

[16]. Merte J, Jensen D, Wright K, Sarsfield S, Wang Y, Schekman R, Ginty DD, Sec24b selectively sorts Vangl2 to regulate planar cell polarity during neural tube closure, Nat Cell Biol, 12 (2009) 41–46; sup pp 41–48. [PubMed: 19966784]

[17]. Guo Y, Zanetti G, Schekman R, A novel GTP-binding protein-adaptor protein complex responsible for export of Vangl2 from the trans Golgi network, Elife, 2 (2013) e00160. [PubMed: 23326640]

[18]. Ma T, Li B, Wang R, Lau PK, Huang Y, Jiang L, Schekman R, Guo Y, A mechanism for differential sorting of the planar cell polarity proteins Frizzled6 and Vangl2 at the trans-Golgi network, J Biol Chem, (2018).

[19]. Iliescu A, Gravel M, Horth C, Gros P, Independent mutations at Arg181 and Arg274 of Vangl proteins that are associated with neural tube defects in humans decrease protein stability and impair membrane targeting, Biochemistry, 53 (2014) 5356–5364. [PubMed: 25068569]

[20]. Iliescu A, Gravel M, Horth C, Kibar Z, Gros P, Loss of membrane targeting of Vangl proteins causes neural tube defects, Biochemistry, 50 (2011) 795–804. [PubMed: 21142127]

[21]. Chien YH, Keller R, Kintner C, Shook DR, Mechanical strain determines the axis of planar polarity in ciliated epithelia, Curr Biol, 25 (2015) 2774–2784. [PubMed: 26441348]

[22]. Andre P, Wang Q, Wang N, Gao B, Schilit A, Halford MM, Stacker SA, Zhang X, Yang Y, The Wnt coreceptor Ryk regulates Wnt/planar cell polarity by modulating the degradation of the core

planar cell polarity component Vangl2, J Biol Chem, 287 (2012) 44518–44525. [PubMed: 23144463]

[23]. Cantrell VA, Jessen JR, The planar cell polarity protein Van Gogh-Like 2 regulates tumor cell migration and matrix metalloproteinase-dependent invasion, Cancer Lett, 287 (2010) 54–61. [PubMed: 19577357]

[24]. Goto T, Davidson L, Asashima M, Keller R, Planar cell polarity genes regulate polarized extracellular matrix deposition during frog gastrulation, Curr Biol, 15 (2005) 787–793. [PubMed: 15854914]

[25]. Williams BB, Cantrell VA, Mundell NA, Bennett AC, Quick RE, Jessen JR, VANGL2 regulates membrane trafficking of MMP14 to control cell polarity and migration, J Cell Sci, 125 (2012) 2141–2147. [PubMed: 22357946]

[26]. Jessen TN, Jessen JR, VANGL2 interacts with integrin alphav to regulate matrix metalloproteinase activity and cell adhesion to the extracellular matrix, Exp Cell Res, 361 (2017) 265–276. [PubMed: 29097183]

[27]. Love AM, Prince DJ, Jessen JR, Vangl2-dependent regulation of membrane protrusions and directed migration requires a fibronectin extracellular matrix, Development, in press (2018).

[28]. Livak KJ, Schmittgen TD, Analysis of relative gene expression data using real-time quantitative PCR and the 2(-Delta Delta C(T)) Method, Methods, 25 (2001) 402–408. [PubMed: 11846609]

[29]. Schmittgen TD, Livak KJ, Analyzing real-time PCR data by the comparative C(T) method, Nat Protoc, 3 (2008) 1101–1108. [PubMed: 18546601]

[30]. Solnica-Krezel L, Schier AF, Driever W, Efficient recovery of ENU-induced mutations from the zebrafish germline, Genetics, 136 (1994) 1401–1420. [PubMed: 8013916]

[31]. Gilmour DT, Jessen JR, Lin S, Manipulating gene expression in the zebrafish, in: Nusslein-Volhard C, Dahm R (Ed.) Zebrafish, a practical approach, Oxford University Press, New York, 2002, pp. 121–143.

[32]. Dray N, Lawton A, Nandi A, Julich D, Emonet T, Holley SA, Cell-fibronectin interactions propel vertebrate trunk elongation via tissue mechanics, Curr Biol, 23 (2013) 1335–1341. [PubMed: 23810535]

[33]. Roszko I, Sepich DS, Jessen JR, Chandrasekhar A, Solnica-Krezel L, A dynamic intracellular distribution of Vangl2 accompanies cell polarization during zebrafish gastrulation, Development, 142 (2015) 2508–2520. [PubMed: 26062934]

[34]. Duperret EK, Dahal A, Ridky TW, Focal-adhesion-independent integrin-alphav regulation of FAK and c-Myc is necessary for 3D skin formation and tumor invasion, J Cell Sci, 128 (2015) 3997–4013. [PubMed: 26359297]

[35]. Ablooglu AJ, Tkachenko E, Kang J, Shattil SJ, Integrin alphaV is necessary for gastrulation movements that regulate vertebrate body asymmetry, Development, 137 (2010) 3449–3458. [PubMed: 20843856]

[36]. Ablooglu AJ, Kang J, Handin RI, Traver D, Shattil SJ, The zebrafish vitronectin receptor: characterization of integrin alphaV and beta3 expression patterns in early vertebrate development, Dev Dyn, 236 (2007) 2268–2276. [PubMed: 17626277]

[37]. Jessen JR, Solnica-Krezel L, Identification and developmental expression pattern of van gogh-like 1, a second zebrafish strabismus homologue, Gene Expr Patterns, 4 (2004) 339–344. [PubMed: 15053985]

[38]. Borovina A, Superina S, Voskas D, Ciruna B, Vangl2 directs the posterior tilting and asymmetric localization of motile primary cilia, Nat Cell Biol, 12 (2010) 407–412. [PubMed: 20305649]

[39]. May-Simera HL, Kai M, Hernandez V, Osborn DP, Tada M, Beales PL, Bbs8, together with the planar cell polarity protein Vangl2, is required to establish left-right asymmetry in zebrafish, Dev Biol, 345 (2010) 215–225. [PubMed: 20643117]

[40]. Kibar Z, Torban E, McDearmid JR, Reynolds A, Berghout J, Mathieu M, Kirillova I, De Marco P, Merello E, Hayes JM, Wallingford JB, Drapeau P, Capra V, Gros P, Mutations in VANGL1 associated with neural-tube defects, N Engl J Med, 356 (2007) 1432–1437. [PubMed: 17409324]

[41]. Lei YP, Zhang T, Li H, Wu BL, Jin L, Wang HY, VANGL2 mutations in human cranial neural-tube defects, N Engl J Med, 362 (2010) 2232–2235. [PubMed: 20558380]

[42]. MacMillan CD, Leong HS, Dales DW, Robertson AE, Lewis JD, Chambers AF, Tuck AB, Stage of breast cancer progression influences cellular response to activation of the WNT/planar cell polarity pathway, Sci Rep, 4 (2014) 6315. [PubMed: 25204426]

[43]. Plow EF, Haas TA, Zhang L, Loftus J, Smith JW, Ligand binding to integrins, J Biol Chem, 275 (2000) 21785–21788. [PubMed: 10801897]

[44]. Conforti G, Calza M, Beltran-Nunez A, Alpha v beta 5 integrin is localized at focal contacts by HT-1080 fibrosarcoma cells and human skin fibroblasts attached to vitronectin, Cell Adhes Commun, 1 (1994) 279–293. [PubMed: 7521757]

[45]. Skubitz AP, Letourneau PC, Wayner E, Furcht LT, Synthetic peptides from the carboxy-terminal globular domain of the A chain of laminin: their ability to promote cell adhesion and neurite outgrowth, and interact with heparin and the beta 1 integrin subunit, J Cell Biol, 115 (1991) 1137–1148. [PubMed: 1955458]

[46]. Baliga BS, Pronczuk AW, Munro HN, Mechanism of cycloheximide inhibition of protein synthesis in a cell-free system prepared from rat liver, J Biol Chem, 244 (1969) 4480–4489. [PubMed: 5806588]

[47]. Heffernan M, Yousefi S, Dennis JW, Molecular characterization of P2B/LAMP-1, a major protein target of a metastasis-associated oligosaccharide structure, Cancer Res, 49 (1989) 6077–6084. [PubMed: 2676155]

[48]. Dang H, Klokk TI, Schaheen B, McLaughlin BM, Thomas AJ, Durns TA, Bitler BG, Sandvig K, Fares H, Derlin-dependent retrograde transport from endosomes to the Golgi apparatus, Traffic, 12 (2011) 1417–1431. [PubMed: 21722281]

[49]. Schaheen B, Dang H, Fares H, Derlin-dependent accumulation of integral membrane proteins at cell surfaces, J Cell Sci, 122 (2009) 2228–2239. [PubMed: 19509052]

[50]. Babst M, Quality control: quality control at the plasma membrane: one mechanism does not fit all, J Cell Biol, 205 (2014) 11–20. [PubMed: 24733583]

[51]. Nagaoka T, Ohashi R, Inutsuka A, Sakai S, Fujisawa N, Yokoyama M, Huang YH, Igarashi M, Kishi M, The Wnt/planar cell polarity pathway component Vangl2 induces synapse formation through direct control of N-cadherin, Cell Rep, 6 (2014) 916–927. [PubMed: 24582966]

[52]. Foot N, Henshall T, Kumar S, Ubiquitination and the Regulation of Membrane Proteins, Physiol Rev, 97 (2017) 253–281. [PubMed: 27932395]

[53]. Patrick GN, Bingol B, Weld HA, Schuman EM, Ubiquitin-mediated proteasome activity is required for agonist-induced endocytosis of GluRs, Curr Biol, 13 (2003) 2073–2081. [PubMed: 14653997]

[54]. Kapp TG, Rechenmacher F, Neubauer S, Maltsev OV, Cavalcanti-Adam EA, Zarka R, Reuning U, Notni J, Wester HJ, Mas-Moruno C, Spatz J, Geiger B, Kessler H, A Comprehensive Evaluation of the Activity and Selectivity Profile of Ligands for RGD-binding Integrins, Sci Rep, 7 (2017) 39805. [PubMed: 28074920]

[55]. Zhang Z, Morla AO, Vuori K, Bauer JS, Juliano RL, Ruoslahti E, The alpha v beta 1 integrin functions as a fibronectin receptor but does not support fibronectin matrix assembly and cell migration on fibronectin, J Cell Biol, 122 (1993) 235–242. [PubMed: 8314844]

[56]. Steele JG, Johnson G, Underwood PA, Role of serum vitronectin and fibronectin in adhesion of fibroblasts following seeding onto tissue culture polystyrene, J Biomed Mater Res, 26 (1992) 861–884. [PubMed: 1376730]

[57]. Galvez BG, Matias-Roman S, Yanez-Mo M, Sanchez-Madrid F, Arroyo AG, ECM regulates MT1-MMP localization with beta1 or alphavbeta3 integrins at distinct cell compartments modulating its internalization and activity on human endothelial cells, J Cell Biol, 159 (2002) 509–521. [PubMed: 12427871]

[58]. Busk M, Pytela R, Sheppard D, Characterization of the integrin alpha v beta 6 as a fibronectin-binding protein, J Biol Chem, 267 (1992) 5790–5796. [PubMed: 1532572]

[59]. Nishimura SL, Sheppard D, Pytela R, Integrin alpha v beta 8. Interaction with vitronectin and functional divergence of the beta 8 cytoplasmic domain, J Biol Chem, 269 (1994) 28708–28715. [PubMed: 7525578]

[60]. Sechler JL, Corbett SA, Schwarzbauer JE, Modulatory roles for integrin activation and the synergy site of fibronectin during matrix assembly, Mol Biol Cell, 8 (1997) 2563–2573. [PubMed: 9398676]

[61]. Dechantsreiter MA, Planker E, Matha B, Lohof E, Holzemann G, Jonczyk A, Goodman SL, Kessler H, N-Methylated cyclic RGD peptides as highly active and selective alpha(V)beta(3) integrin antagonists, J Med Chem, 42 (1999) 3033–3040. [PubMed: 10447947]

[62]. Boettiger D, Lynch L, Blystone S, Huber F, Distinct ligand-binding modes for integrin alpha(v)beta(3)-mediated adhesion to fibronectin versus vitronectin, J Biol Chem, 276 (2001) 31684–31690. [PubMed: 11423542]

[63]. Boettiger D, Huber F, Lynch L, Blystone S, Activation of alpha(v)beta3-vitronectin binding is a multistage process in which increases in bond strength are dependent on Y747 and Y759 in the cytoplasmic domain of beta3, Mol Biol Cell, 12 (2001) 1227–1237. [PubMed: 11359918]

[64]. De Franceschi N, Hamidi H, Alanko J, Sahgal P, Ivaska J, Integrin traffic - the update, J Cell Sci, 128 (2015) 839–852. [PubMed: 25663697]

Highlights

- Integrin αv regulates VANGL2 protein levels *in vitro* and in zebrafish
- Integrin β3 and β5 have opposing effects on VANGL2 protein
- Integrin activation stabilizes VANGL2 protein
- Inhibition of cell-matrix adhesion reduces VANGL2 protein

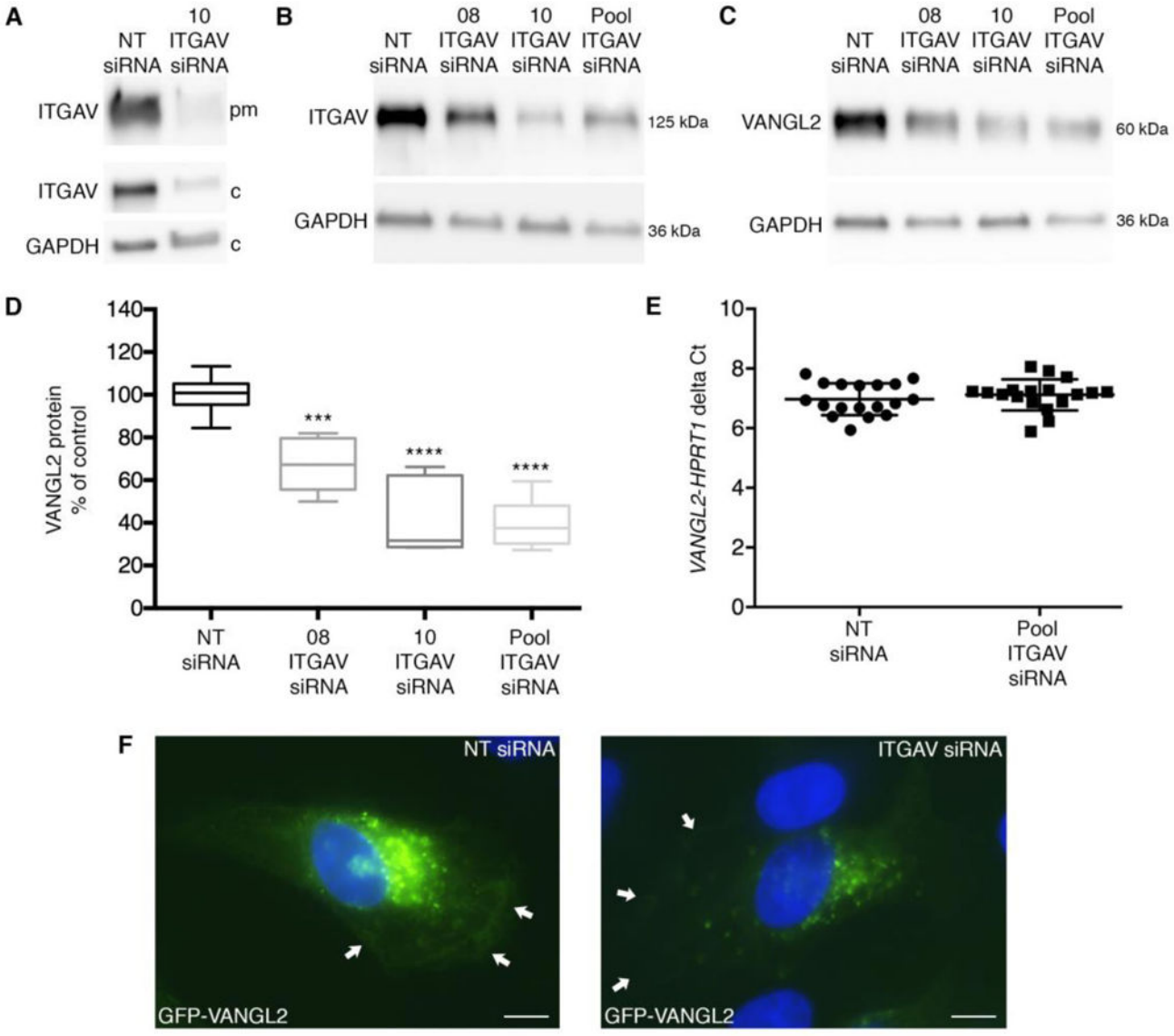

Fig. 1.

Integrin αv regulates VANGL2 protein levels but not transcription. (**A**) Western blot of biotinylated plasma membrane (pm) and cytoplasmic (c) integrin αv (ITGAV) protein from non-targeting (NT) control and single (#10) integrin αv siRNA transfected HT-1080 cells. (**B**) Western blot of total protein from NT control and integrin αv knockdown cells. #08 is a single siRNA to integrin αv and the pool is a mixture of four integrin αv siRNAs that includes 08 and 10. (**C**,**D**) Integrin αv knockdown cells have reduced total VANGL2 protein levels. Box plots show median value ± standard deviation (whiskers) and the interquartile range (boxes) of likely variation (experiment performed three times, n = 6 biological replicates). (**E**) Quantitative RT-PCR was performed using TaqMan probes for *HPRT1* and *VANGL2* and cDNA obtained from NT control and integrin αv siRNA transfected cells. Scatter plot of delta Ct values (*VANGL2-HPRT1* delta Ct) showing the average value ± standard deviation (experiment performed three times, n = 18 biological replicates). (**F**)

GFP-VANGL2 expression in NT control and integrin αv siRNA transfected cells shown under identical imaging parameters. Arrows denote plasma membrane expression. The integrin αv image was brightened to allow accurate arrow placement and then reduced to the original parameters. ***$P < 0.001$; ****$P < 0.0001$; P values are versus NT siRNA in panel **D**; two-tailed unpaired t-test. Scale bars = 5 μm.

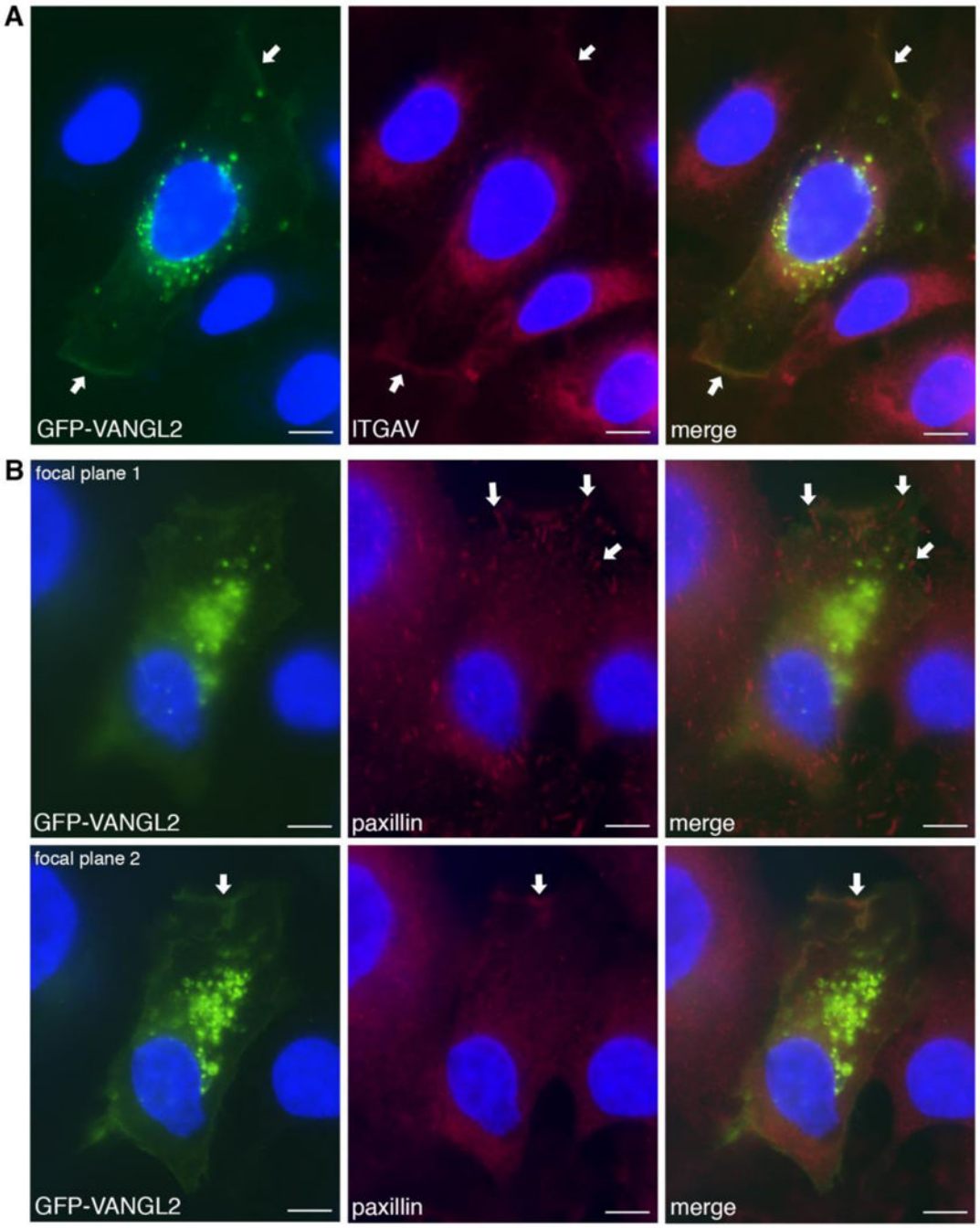

Fig. 2.

GFP-VANGL2 co-localizes with integrin αv at the plasma membrane. (**A**) GFP-VANGL2 transfected HT-1080 cells immunolabeled using an integrin αv (ITGAV) antibody show co-labeling at the plasma membrane (white arrows). (**B**) GFP-VANGL2 transfected cells immunolabeled using a paxillin antibody. At focal plane 1, paxillin-positive focal adhesions were observed that lack GFP-VANGL2 expression (white arrows). At focal plane 2, GFP-VANGL2 co-localizes with paxillin at certain plasma membrane domains (white arrows). Scale bars = 5 μm.

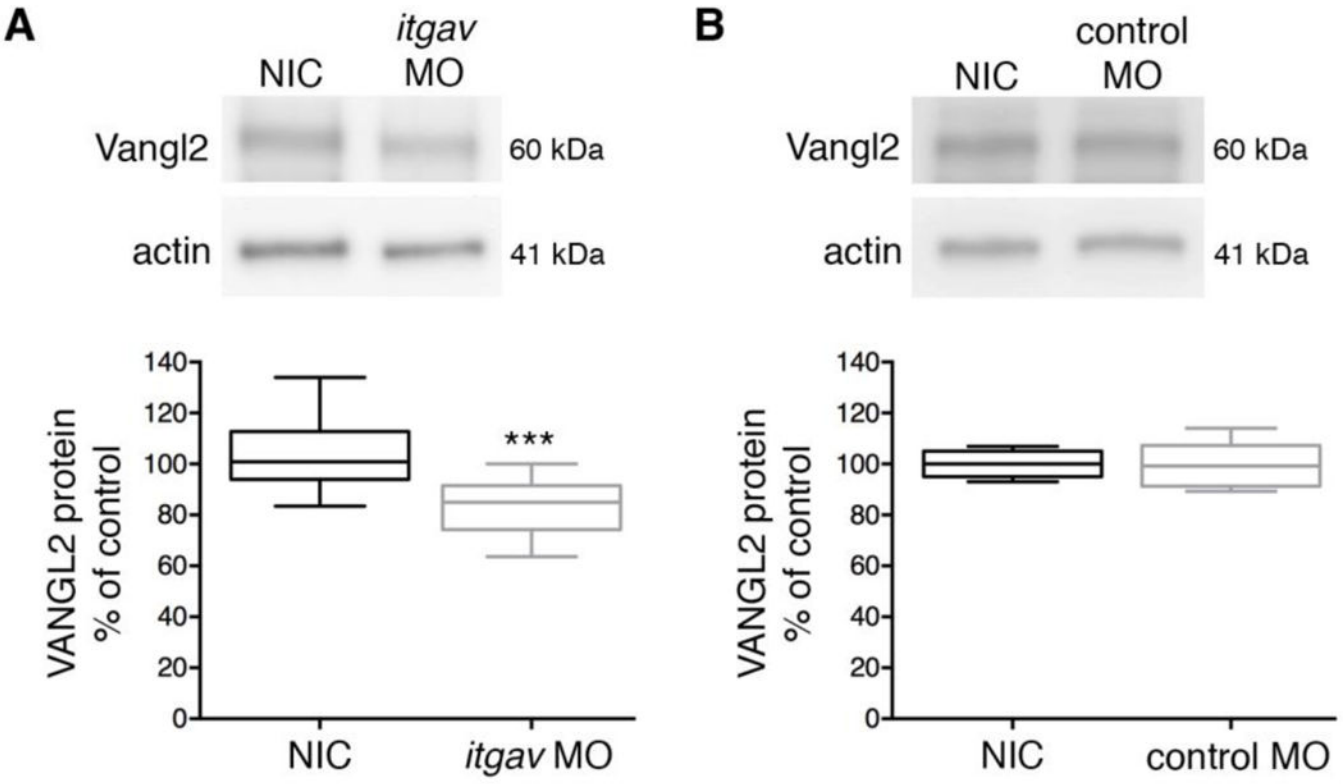

Fig. 3.

Integrin αv knockdown reduces Vangl2 protein in zebrafish. (**A**) Western blot of total protein from 24 h post-fertilization embryos. Protein was extracted from non-injected control (NIC) and *integrin αv* (*itgav*) morpholino (MO) injected wild-type embryos. (**B**) Western blot of total protein isolated from non-injected and standard control morpholino injected wild-type embryos. (**A**,**B**) Box plots show median value ± standard deviation (whiskers) and the interquartile range (boxes) of likely variation (experiment performed three times, n = 13 biological replicates). Injection of integrin αv morpholino caused a 20% average reduction in Vangl2 protein levels. ***$P < 0.001$; P value is versus NIC; two-tailed unpaired t-test.

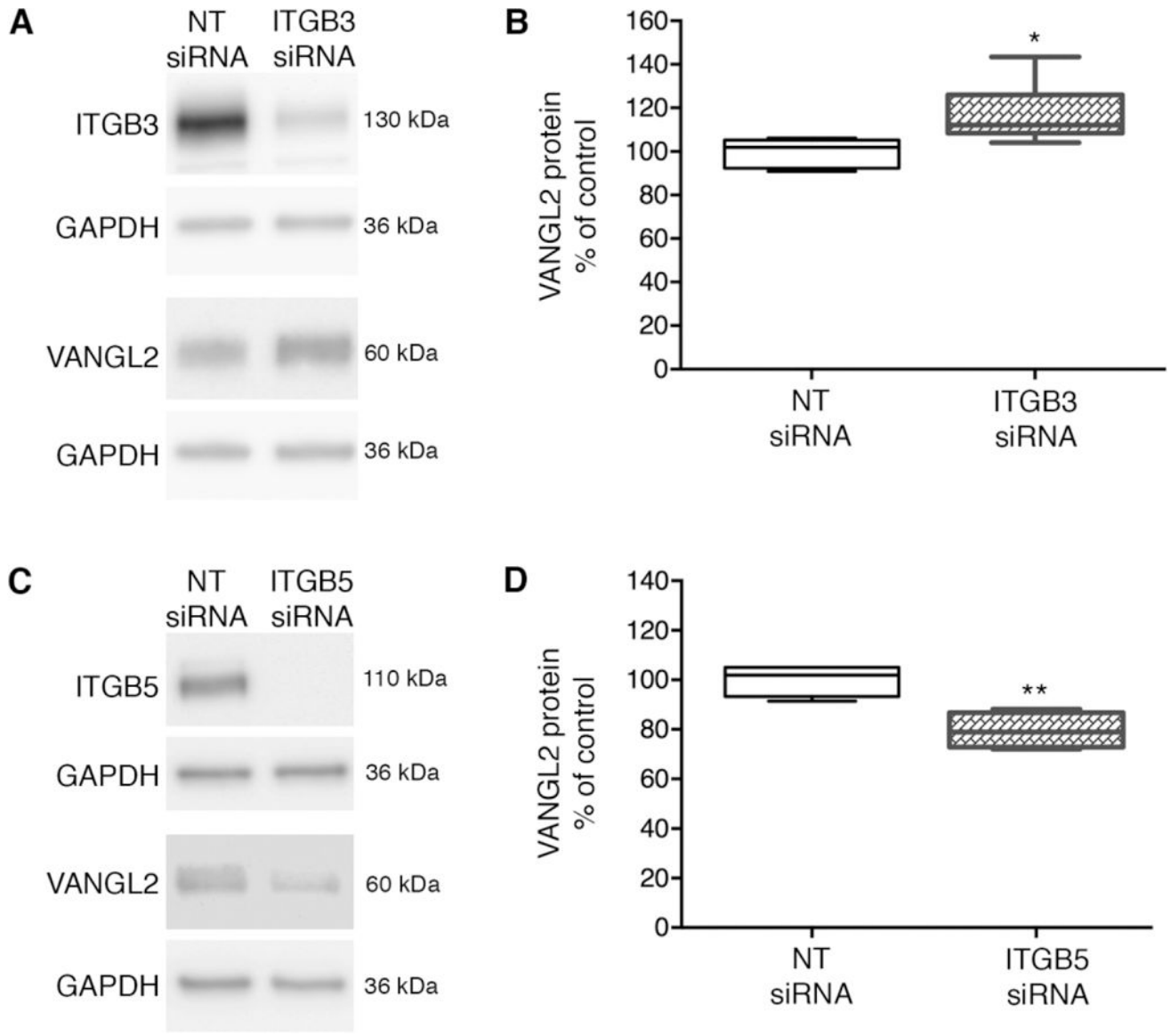

Fig. 4.

Opposing effects of integrin β3 and integrin β5 knockdown on VANGL2 protein levels.(A) Western blots of total protein from non-targeting (NT) control and integrin β3 (ITGB3) knockdown HT-1080 cells. Integrin β3 protein is reduced by 89%. (**B**) Box plot shows median value ± standard deviation (whiskers) and the interquartile range (boxes) of likely variation. Integrin β3 knockdown cells have increased VANGL2 protein levels (experiment performed three times, n = 9 biological replicates). (**C**) Western blots of total protein from NT control and integrin β5 knockdown cells. Integrin β5 protein is reduced by 100%. (**D**) Box plot showing integrin β5 knockdown cells have decreased VANGL2 protein levels (experiment performed three times, n = 8 biological replicates). *$P < 0.05$; **$P < 0.01$; P values are versus NT siRNA; two-tailed unpaired t-test.

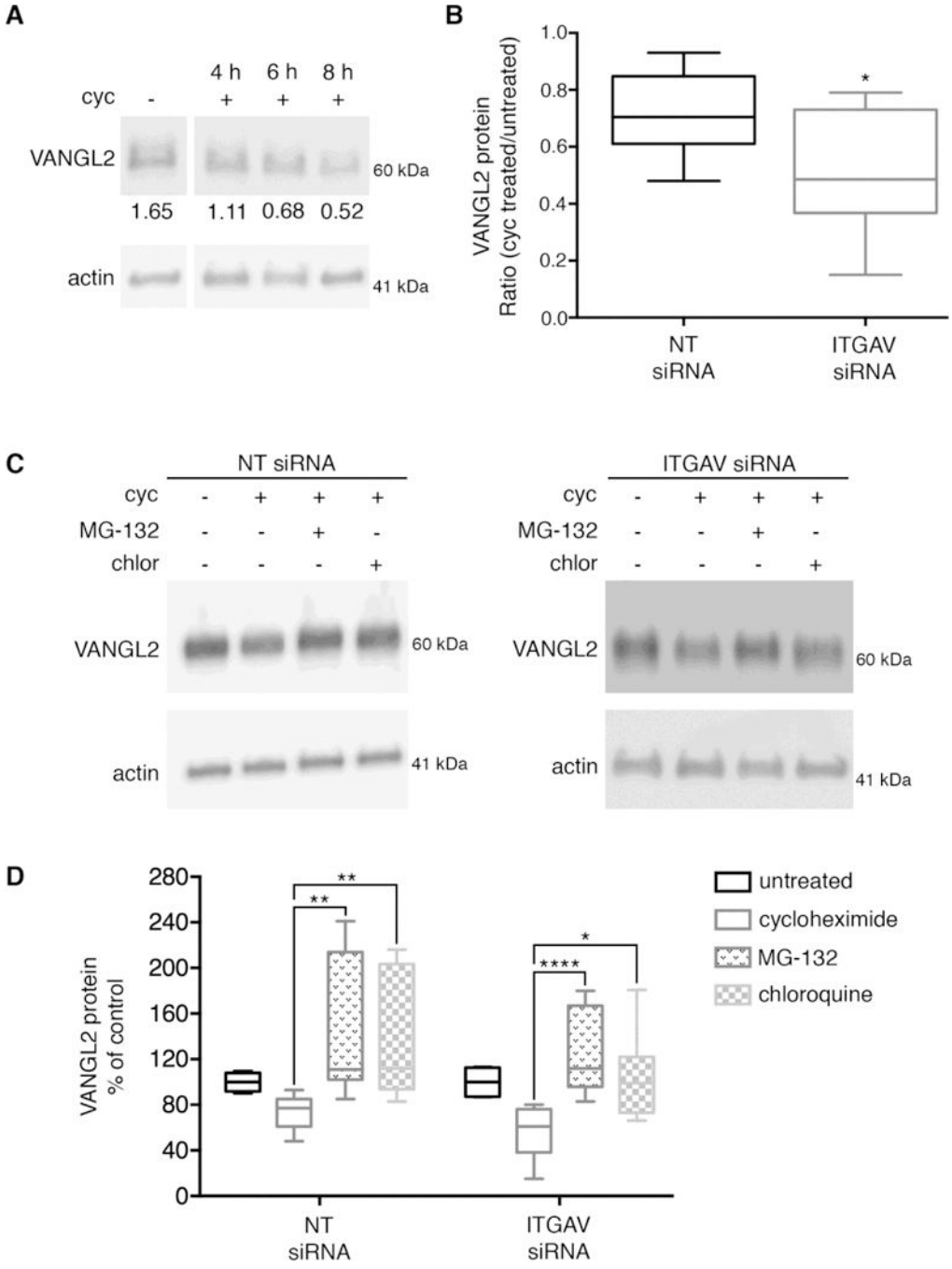

Fig. 5.

VANGL2 protein degradation is regulated by integrin αv. (**A**) Western blot of total protein from HT-1080 cells that were untreated or treated with cycloheximide (cyc) as indicated (experiment performed three times, n = 3 biological replicates). Densitometry numbers for VANGL2 are normalized to actin. (**B**) Box plot shows the ratio of VANGL2 protein in cyc treated/untreated non-targeting (NT) control and integrin αv (ITGAV) siRNA transfected HT-1080 cells (experiment performed three times, n = 11 biological replicates). The median value ± standard deviation (whiskers) and the interquartile range (boxes) are shown. (**C**)

Western blots of total protein from NT and integrin αv knockdown cells untreated and treated with cycloheximide, MG-132, or chloroquine (chlor). These data were used to generate the box plots shown in panels **B** and **D**. (**D**) Box plot showing reduced VANGL2 protein levels in integrin αv knockdown cells are rescued by both MG-132 and chloroquine treatment (experiment performed three times, n = 8 biological replicates). *$P < 0.05$; **$P < 0.01$; ****$P < 0.0001$; P values are versus NT siRNA in panel **B** and as indicated in panel **D**; two-tailed unpaired t-test.

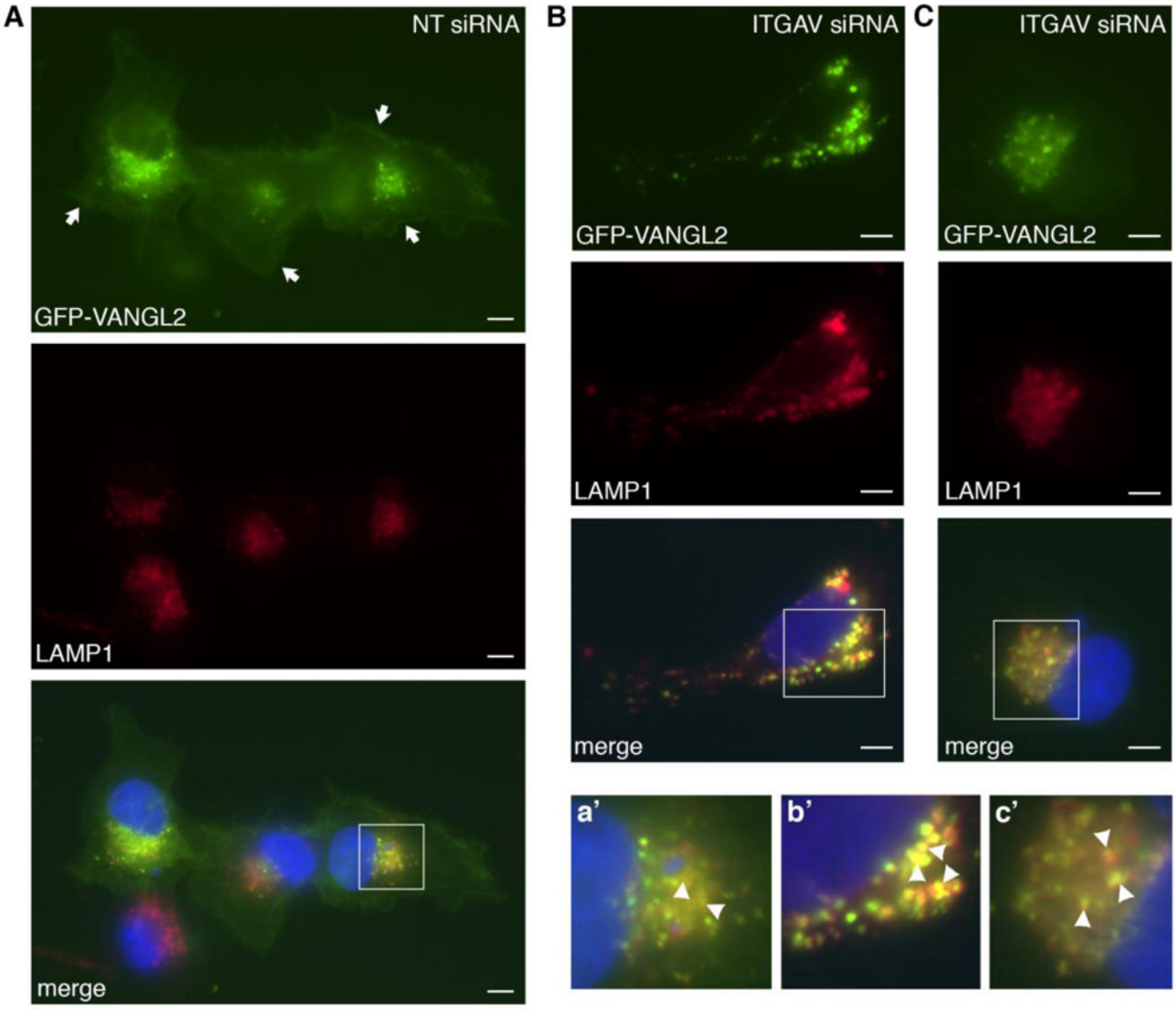

Fig. 6.

Lysosomal VANGL2 localization in integrin αv knockdown cells. (**A**) Non-targeting (NT) control siRNA transfected cells expressing GFP-VANGL2 and immunolabeled for LAMP1. Nuclei are labeled with DAPI (blue). Arrows denote plasma membrane expression. (**B**,**C**) Integrin αv (ITGAV) siRNA transfected cells expressing GFP-VANGL2 and with LAMP1 and DAPI labeling. **a'-c'** Enlarged images of white-boxed regions in panels **A**-**C**. Certain double-positive vesicles are highlighted with arrowheads. Scale bars = 5 μm.

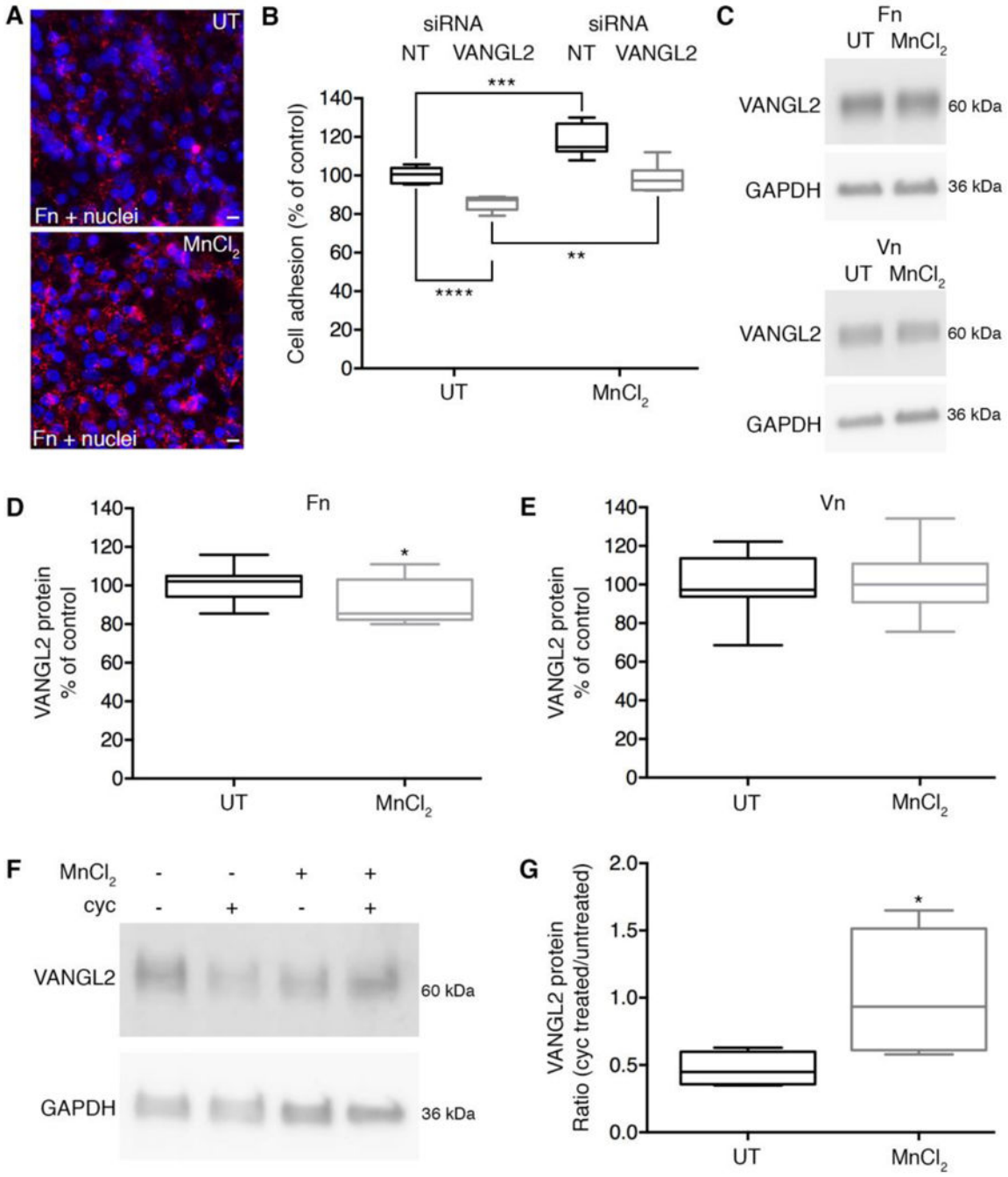

Fig. 7.

Integrin activation stabilizes VANGL2 protein levels. (**A**) Fibronectin (Fn) immunolabeling of HT-1080 cells untreated (UT) or treated with $MnCl_2$ to stimulate integrin activation and fibronectin assembly. Nuclei are labeled with DAPI (blue). Scale bars = 20 μm.(B) Box plot of cell adhesion assay data showing effect of $MnCl_2$ treatment on non-targeting (NT) control and VANGL2 siRNA transfected cells (experiment performed three times, n = 6 biological replicates). The median value ± standard deviation (whiskers) and the interquartile range (boxes) are shown. (**C**) Western blots of VANGL2 expression in untreated and $MnCl_2$

treated cells plated on fibronectin and vitronectin. (**D**,**E**) Box plots showing VANGL2 protein levels are not increased in $MnCl_2$ treated cells (experiments performed three times, n = 12 biological replicates). (**F**) Western blot of VANGL2 expression in cells that were untreated or treated with $MnCl_2$ and/or cycloheximide (cyc). (**G**) Box plot showing the ratio of VANGL2 protein in cycloheximide treated/untreated cells with and without $MnCl_2$ (experiment performed 6 times, n = 6 biological replicates). *$P < 0.05$; **$P < 0.01$; ***$P < 0.001$; ****$P < 0.0001$; P values are as indicated in panel **B** and versus VANGL2 expression in untreated cells in panels **D** and **G**; two-tailed unpaired *t*-test.

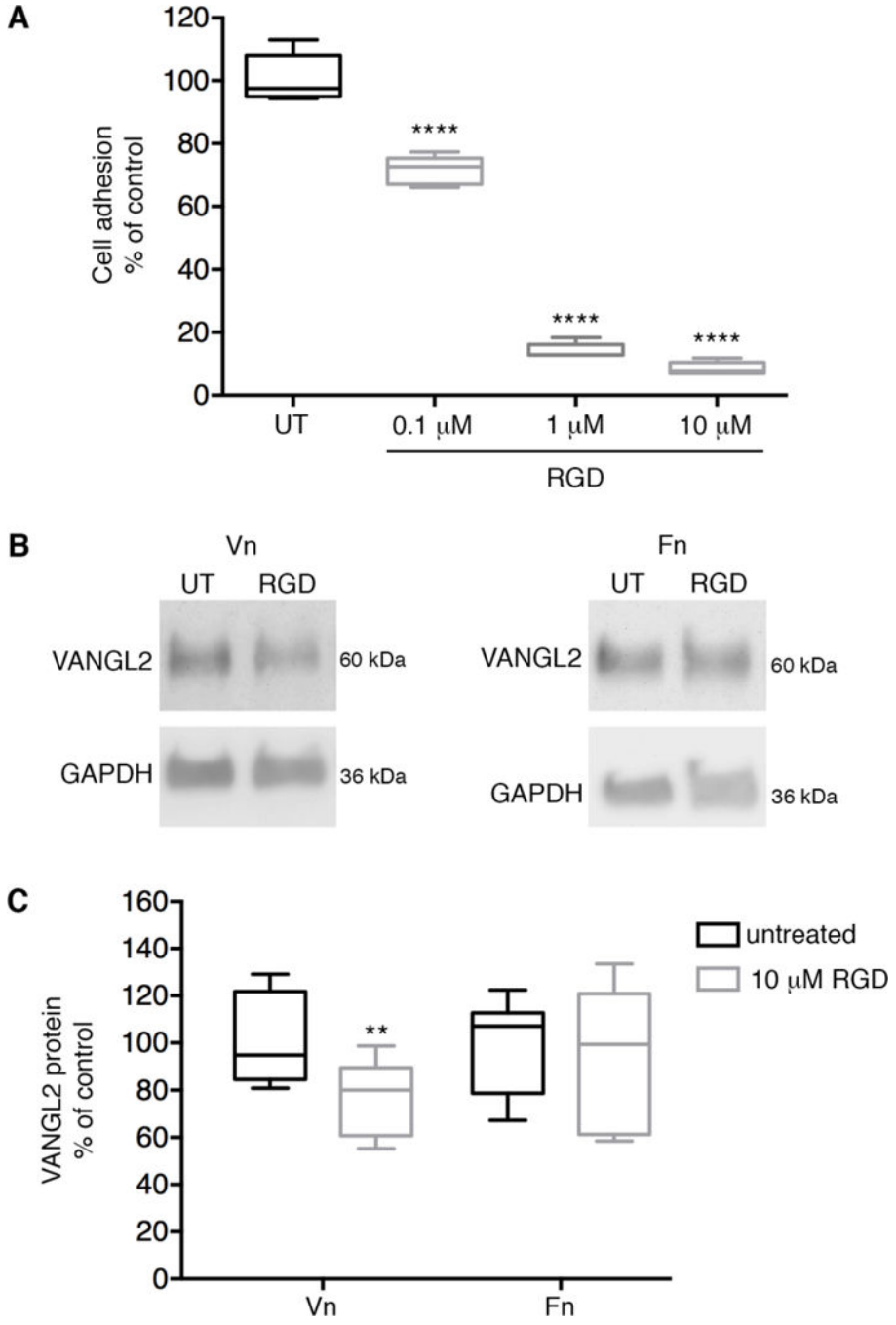

Fig. 8.

Inhibition of cell-matrix adhesion reduces VANGL2 protein levels. (**A**) Box plot of HT-1080 vitronectin cell adhesion assay data showing effect and titration of RGD peptide treatment. The median value ± standard deviation (whiskers) and the interquartile range (boxes) are shown.(**B**) Western blots of untreated (UT) and RGD peptide treated cells plated on vitronectin (Vn) and fibronectin (Fn). (**C**) Box plot showing VANGL2 protein levels are decreased when integrin-vitronectin adhesion is inhibited (experiment performed four times,

n = 10 biological replicates).** $P < 0.01$; **** $P < 0.0001$; P values are versus untreated cells; two-tailed unpaired t-test.